J Therm Anal Calorim (2016) 124:1727–1734
DOI 10.1007/s10973-016-5284-2

Thermal reaction mechanisms of nano- and micro-scale aluminum powders in carbon dioxide at low heating rate

Yunlan Sun[1] · Rong Sun[1] · Baozhong Zhu[1] · Keke Mao[1] · Yuxin Wu[1]

Received: 4 October 2015 / Accepted: 17 January 2016 / Published online: 4 February 2016

Abstract Thermal reaction mechanisms of nano- and micro-scale aluminum powders with a mean particle diameter of 50 nm and 1–2 μm were investigated by a thermogravimetric analysis coupled with a differential scanning calorimetry. Thermal reaction characteristics of nano-scale aluminum powder are significantly different from that of micro-scale aluminum powder. The key reaction of nano-scale aluminum powder takes place in the low-temperature region, while for micro-scale aluminum powder, the key reaction takes place in the high-temperature region. Scanning electron microscopy and X-ray diffraction were also conducted to analyze the thermal reaction products. There is a striking difference for the thermal reaction products, which are the oxide shell disruption of micro-scale aluminum particles. X-ray diffraction patterns indicate that γ-Al_2O_3 is detected before aluminum melting point for nano-scale aluminum powder, but for micro-scale aluminum powder, γ-Al_2O_3 is detected after aluminum melting point. Alumina crystal structures of nano- and micro-scale aluminum powders are different at different mass gain stages. The sequence of the products of nano- and micro-scale aluminum powders is amorphous oxide $\rightarrow \gamma \rightarrow \alpha$-$Al_2O_3$ and amorphous oxide $\rightarrow \gamma \rightarrow \theta \rightarrow \alpha$-$Al_2O_3$, respectively. Furthermore, thermal reaction mechanisms of nano- and micro-scale aluminum powders are discussed at a low heating rate.

Keywords Thermal reaction mechanism · Nano-scale aluminum · Micro-scale aluminum · Carbon Dioxide

✉ Baozhong Zhu
baozhongzhu@163.com

[1] School of Energy and Environment, Anhui University of Technology, Ma'anshan 243002, Anhui, China

Introduction

Aluminum (Al) powder, as a very common energetic material, is widely used in propellants [1] and nano-composite metal materials [2]. It increases the specific impulse of the propellant by increasing combustion temperature in the solid rocket motor and decreasing the molecular weight of products [3]. In addition, there is a high amount of Al on the earth, which results to a lower cost of Al mining. However, the formed solid oxide would adhere on the surface of metal particles and make the combustion process of metal more complex than that of hydrocarbon fuels.

Particle diameter is one of the factors that affect the combustion process of Al powder. In order to understand the combustion processes of nano- and micro-scale Al powders, several experiments were performed on the Al powder combustion. The results showed that nano-scale Al particle clouds burnt faster than micro-scale Al particle clouds in air [4]. Yan [5] showed that the melting enthalpy and melting temperature of Al powder decreased with the decreases in Al particles size. Moreover, nano-scale Al particle has more attractive oxidation energetics and fast reaction kinetics than micro-scale or larger Al particles [6]. All these results showed the different reaction characteristics between nano- and micro-scale Al powders.

In addition, there were some studies on the reaction characteristics of Al in dry air [7–9] and various mixed environments [10–13], but few studies carried out on thermal reaction characteristics of Al powder in carbon dioxide (CO_2) atmosphere [14, 15]. The reaction of Al and CO_2 releases large amounts of energy. On the other hand, Martian atmospheres consist of 95 % CO_2, making the achievement of in situ resource utilization (ISRU)

possible. Therefore, Al/CO_2 is regarded as a promising fuel to realize an exploration mission to Mars in the future. However, there is little knowledge about the reaction of Al powder and CO_2, so it would be conducive to the development of Mars exploration if the thermal reaction mechanism of Al powder and CO_2 is clarified.

In this paper, thermal reaction characteristics of nano- and micro-scale Al powders were studied by a thermogravimetric analyzer coupled with a differential scanning calorimetry (TG-DSC) which were widely used and well-understood. Scanning electron microscopy (SEM) was also used to observe the morphology of thermal reaction products of Al powder. And the components of products were studied by X-ray diffraction (XRD). At the same time, thermal reaction mechanisms of nano- and micro-scale Al powders were inferred.

Experimental

Al powder used in the present work was provided by Nanometer Material Limited Company in Henan province. The average diameters of micro- and nano-scale Al powders were 1–2 μm and 50 nm, respectively. The corresponding active Al contents measured by chemical method [16] were 94.0 and 82.0 %, respectively.

Oxidation of Al powder was studied using a Netzsch STA 449C simultaneous TG-DSC thermal analyzer. Thermogravimetric analysis (TG) was used to measure the sample mass gain and the indicative of the oxidation when Al powder was heated in CO_2 atmosphere. Heat flux of Al powder was studied by DSC. Al powder with a mass range of 4–6 mg was heated at the heating rate of 10 °C min^{-1} from 20 to 1400 °C under atmospheric pressure conditions, and CO_2 (99.99 %) was used as the oxidant. Reaction gas (CO_2) flow and protective gas (CO_2) flow were controlled at 40 and 10 mL min^{-1}, respectively. In addition, both TG and DSC baselines were corrected by subtraction of predetermined baselines run under identical conditions except for the absence of sample.

The thermal reaction products of Al powder quenched at different particular temperature were collected when the samples were cooled down to the room temperature. The morphology of product which was quenched at 1400 °C was observed by FEI scanning electron microscopy (SEM) (Model-NOVA NANO SEM430). And components of products quenched at different temperatures were analyzed by Bruker X-ray diffractometer (XRD) (Model-D8 ADVANCE, CuKa, $\lambda = 1.54187$).

Results and discussion

Thermal reaction characteristics of nano- and micro-scale Al powders

It can be seen from Fig. 1 that the oxidation of nano-scale Al powder and CO_2 can be divided into two primary stages: induction stage and mass gain stage. There is no mass gain from 20 to 470 °C, called induction stage. After the induction stage, there is a stage of mass gain that can be further divided into three substages. The first mass gain is observed at 470–690 °C, which is called stage I. The second mass gain ranges from 690 to 875 °C which is called stage II. Stage III is found at 875–1136 °C. However, there are a few mass losses when the temperature is above 1136 °C. Actually, whether in wet or dry CO_2, carbon can be produced in the reaction between aluminum and CO_2 [17]. The reaction between C and CO_2 (Boudouard reaction) takes place when the reaction temperature is above

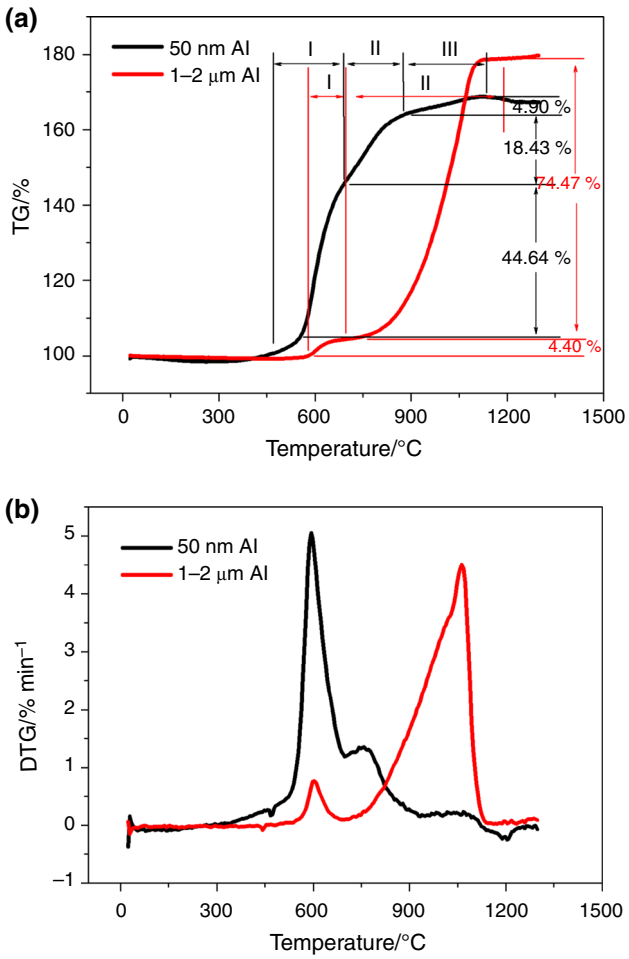

Fig. 1 Thermal analysis patterns of nano- and micro-scale Al powders. **a** TG curves; **b** DTG curves

1000 °C [18]. Therefore, the tail of TG curve of nano-scale Al powder drops down after 1136 °C due to the Boudouard reaction ($C(s) + CO_2(g) \rightarrow 2CO(g)$).

Thermal reaction of micro-scale Al powder and CO_2 can be also divided into two major stages: induction stage and mass gain stage. Mass gains from 20 to 579 °C are not detected at the induction stage. As for mass gain stage of micro-scale Al powder, compared with three substages of nano-scale Al powder, it can be divided into two substages. The first mass gain is observed at 579–697 °C, which is called stage I. The second mass gain ranges from 697 to 1188 °C, which is called stage II.

In order to compare the differences of mass gain between nano- and micro-scale Al powders, the mass gains of each stage are shown in Table 1. The mass gains of stage I, stage II, and stage III are represented by Δm_{I}, Δm_{II}, and Δm_{II}, respectively. It can be obtained by the Eq. (1), where m is the mass at the end of each stage and m_o is the initial mass.

$$\Delta m = \frac{m - m_{\mathrm{o}}}{m_{\mathrm{o}}} \tag{1}$$

As shown in Table 1, the mass gain of nano-scale Al powder is 44.64 % at stage I, which means that the key reaction takes place at a low temperature for nano-scale Al powder. This result is consistent with the Ref. [19]. And the mass gains of stages II and III reduce gradually. Especially for stage III, there is only 4.90 % mass gain. For micro-scale Al powder, there is only 4.40 % mass gain at stage I. However, mass gain at stage II is 74.47 %, which indicates that the key reaction of micro-scale Al powder takes place at stage II.

DSC curves of nano- and micro-scale Al powders are shown in Fig. 2, and an endothermic peak around 660 °C is detected, which corresponds to the melting point of Al. Generally, onset temperature of extrapolated peak is used to define the melting point, causing the less dependence of extrapolated onset temperature on heating rate, thermal conductivity of sample, thickness of sample, and mass of sample compared with the peak temperature [20]. Thus, according to the extrapolation method, the melting points of nano- and micro-scale Al powders in this study are 652.6 and 654.0 °C, respectively. The melting point of nano-scale Al powder is slightly lower than that of micro-scale Al powder, which is consistent with the results that the melting temperature decreases with the decrease in Al particle size [5, 21]. In addition, the melting enthalpies of nano- and micro-scale Al powders are 33.42 and 250.6 J g^{-1}, respectively, by calculating the melting peak area. This result indicates that the melting enthalpy also decreases with the decrease in Al particle size. It is worth noting that the melting enthalpy (melting endothermic peak) of nano-scale Al powder is smaller than that of micro-scale Al powder due to the exothermic oxidation of nano-scale Al powder at a low temperature, so there is a deep impact of particle size on the melting behavior of Al. In order to further understand the influence of particle size on melting behavior of Al powder, the mass gains of Al powder before the melting point and during the whole reaction are calculated, represented by $\Delta m'$ and $\Delta m''$, respectively. The results are shown in Table 2.

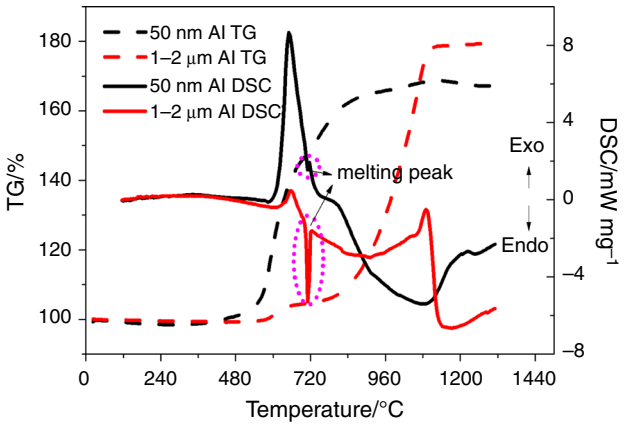

Fig. 2 TG–DSC curves of nano- and micro-scale Al powders at a heating rate of 10 °C min^{-1}

It can be noted from Table 2 that the mass gains of nano-scale Al powder before the melting temperature ($\Delta m'$) are far higher than those of micro-scale Al powder. Furthermore, mass gains of nano-scale Al powder before the melting point are relatively higher than those of the whole reaction. The results show that the key reaction of nano-scale Al powder takes place before the melting point, which means the solid form of Al powder that involves in oxidation. However, for micro-scale Al powder, the mass gains before the melting point are only 4.38 %, which is far lower than 78.87 % mass gains of the whole reaction. This shows that the key reaction of micro-scale Al powder takes place between molten Al and CO_2.

Table 1 Mass gains of each stage for nano- and micro-scale Al powders

Sample	Δm_{I}/%	Δm_{II}/%	Δm_{III}/%
50 nm	44.64	18.43	4.90
1–2 μm	4.40	74.47	–

Table 2 Mass gains of nano- and micro-scale Al powders before the melting point and during the whole reaction

Sample	$\Delta m'$/%	$\Delta m''$/%
50 nm	42.18	67.97
1–2 μm	4.38	78.87

Morphology of residuals

Figure 3a indicates the morphology of the residuals of nano-scale Al powder. It can be seen from Fig. 3a that the residuals are like corals which consist of irregular particles. And the main size of the residuals of Al particle is greater than 50 nm, the mean size of initial particles. According to the diffusion mechanisms, the volume increases when Al is oxidized to alumina [19], so the oxidation of nano-scale Al powder is consistent with a shrink core-type model [3].

Figure 3b shows the morphology of the residuals of micro-scale Al powder. As can be seen from Fig. 3b, a number of larger globular particles are formed due to the aggregation of Al particles. It can be also easily found that some fragments with a rough outer surface appear. In addition, the inner surface of the fragment is also rough, which is marked with a red circle shown in Fig. 4. It can be found that some holes are formed on the spherical particles.

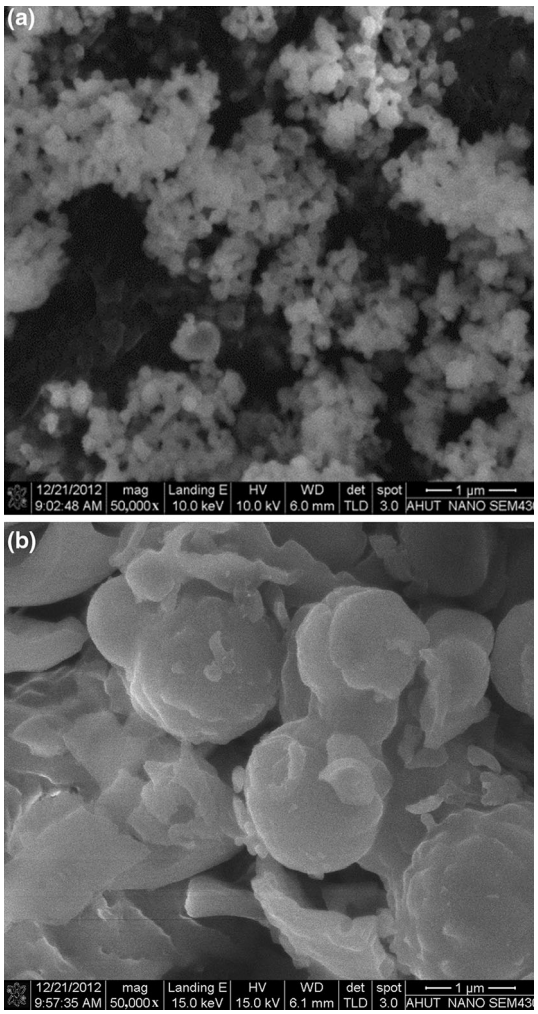

Fig. 3 SEM images of residuals after heated to 1400 °C. **a** Nano-scale Al powder; **b** micro-scale Al powder

The results show that the formation of fragments and holes can be explained by changes in pressure in Al core, between Al core and alumina. The melting of Al is accompanied by a 6 % volume increase due to the decreases in density from 2.7 to 2.4 g cm^{-3}, which causes a compressive pressure within the Al core [22]. This high tensile stress leads to the shell's dynamic fracture and spallation. Mechanical stress at the interface between the metal and oxide results in an increase in the reaction rate followed by the disruption of the film. Thus, the differences in the thermal expansion coefficients and densities of the metal and its oxide, as well as in the volume change in metal during phase or polymorphic transformations, are responsible for these fragments. In addition, the produced CO gases disrupt the oxide shell caused by the expansion of them and the holes are formed. If the amount of produced CO gas is very large and the space of the oxide coatings is small, hollow oxide shells of particles form as fragments from brittle fracturing of the thin walls due to the expansion of CO gas and aluminum core.

Components of residuals

The phase transformation of alumina film on Al particle surface by thermal oxidation was established by Levin [23], and the sequence of alumina phase transformations shown in Ref. [23] is amorphous $\rightarrow \gamma \rightarrow \delta \rightarrow \theta \rightarrow \alpha$-$Al_2O_3$. Amorphous alumina is thermodynamically more stable than crystalline alumina [24]. The thickness of amorphous alumina layer increases with temperature increasing until it reaches a critical value [5, 24]. And then the transformation of amorphous alumina to a crystalline alumina polymorph takes place.

In order to understand the thermal reaction mechanisms of nano- and micro-scale Al powders with CO_2 and to

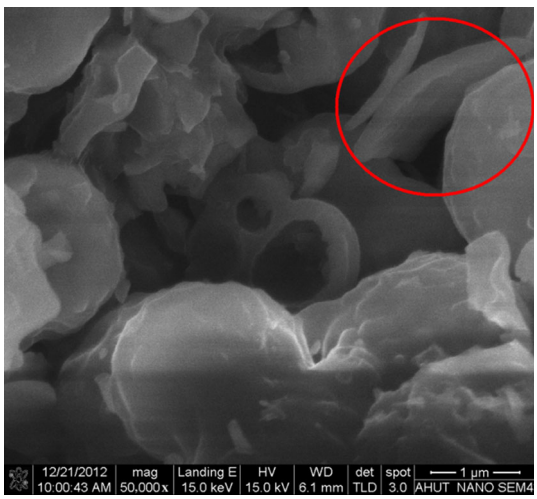

Fig. 4 SEM image of micro-scale Al powder after heated to 1400 °C

identify intermediate products, several Al samples were heated in CO_2 at 10 °C min^{-1} to selected temperatures in this paper. And then the products quenched at selected temperature were analyzed by X-ray diffraction. The results are shown in Fig. 5.

The initial nano- and micro-scale Al powders (at 25 °C) were also analyzed by XRD as shown in Fig. 5. Although only diffraction peaks of Al for initial Al powder are detected, there may be some amorphous Al_2O_3, because amorphous Al_2O_3 could be hardly detected by XRD. After being heated to 600 °C, the formed alumina phases are referred to as γ-Al_2O_3 for nano-scale Al powder, which corresponds to stage I. This result shows that the polymorph of alumina phase presents as γ-Al_2O_3 in the reaction between nano-scale Al powder and CO_2 before the Al melting point. When the temperature increases to 800 °C, peaks of γ-Al_2O_3 become stronger. This means the growth of γ-Al_2O_3 with temperature increasing. The γ-Al_2O_3 layer eventually transforms into α-Al_2O_3 at 1200 °C. Note that no θ-Al_2O_3 or δ-Al_2O_3 is detected at the changing of alumina crystal. It is consistent with the reports [23, 25] that the transformation of γ-Al_2O_3 to α-Al_2O_3 may proceed directly or via a number of intermediate phases.

For micro-scale Al powder, there are also some diffraction peaks of Al at 25 °C. At 600 °C, no new alumina crystal is found, and only diffraction peaks of Al are present. Weak diffraction peaks of γ-Al_2O_3 can be detected after being heated to 800 °C. When the temperature increases to 1000 °C, θ-Al_2O_3 is found and diffraction peaks of γ-Al_2O_3 become stronger. As the reaction temperature increases, strong diffraction peaks of α-Al_2O_3 are observed at 1400 °C, which indicates the formation of stable Al_2O_3 crystal. Thus, the transformation sequence of alumina film is amorphous → $\gamma \rightarrow \theta$ → α-Al_2O_3.

As discussed above, it can be concluded that the main alumina crystal in products of the first, second, and third mass gains for nano-scale Al powder is γ-Al_2O_3, γ-Al_2O_3, and α-Al_2O_3, respectively. And for micro-scale Al powder, the main crystal of alumina phase at stage I may be amorphous Al_2O_3. However, at stage II, it has changed greatly, such as amorphous oxide → γ-Al_2O_3 or θ-Al_2O_3.

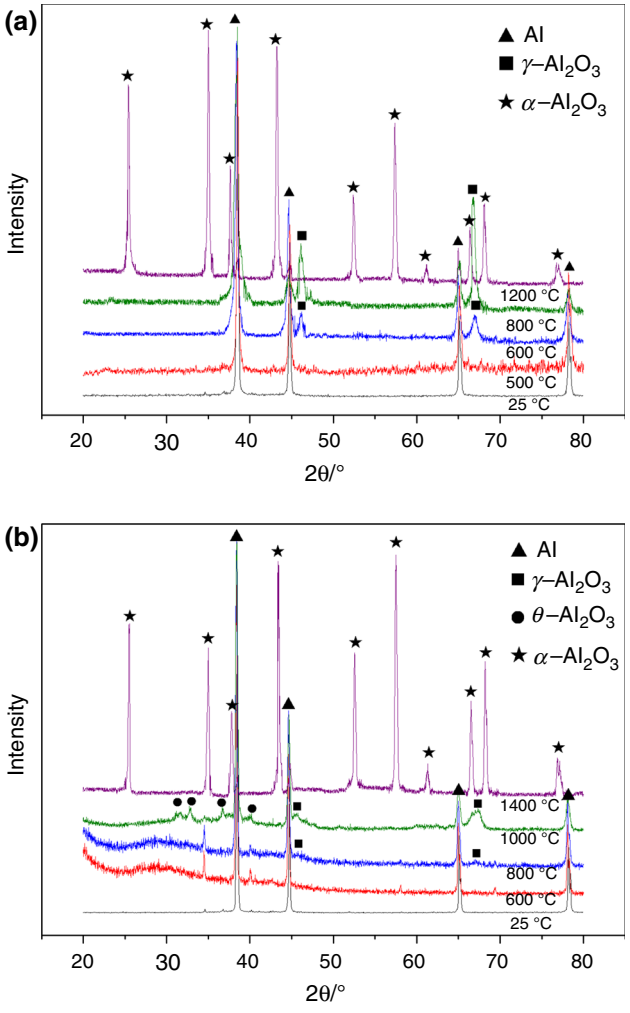

Fig. 5 XRD patterns of Al particles at different quenched temperatures. **a** 50 nm Al; **b** 1–2 μm Al

Thermal reaction mechanisms

Thermal reaction mechanisms of nano-scale Al powder

During induction stage (20–470 °C), there are no obviously mass gains of Al powder. This shows the existence of an integrated protective Al_2O_3 layer that adheres to Al particles, which is known as amorphous alumina [23]. As temperature increases, the thickness of amorphous alumina layer increases. The rate of this process is controlled by the outward diffusion of Al cations [26]. TG curve is the evidence of a slow oxidation of Al powder at induction stage. For the fast oxidation, oxidation process is illustrated in Fig. 6. As shown in Fig. 6, a large number of CO_2 molecules penetrate the Al_2O_3 shell and the particle's diameter becomes larger with the oxidation of nano-scale Al particle. When thickness of the oxide layer exceeds the critical thickness of amorphous alumina, the oxide transforms into γ-Al_2O_3 whose density is about 20 % higher than that of amorphous Al_2O_3. At the beginning of transformation, the smallest crystallite size of γ-Al_2O_3 has been found to be in the range of a few nanometers comparable with the thickness of oxide layer existing at this point on the Al surfaces [23]. Thus, it is suggested that the newly formed γ-Al_2O_3 partially covers the Al particle which is previously isolated by a continuous amorphous Al_2O_3 shell. Then,

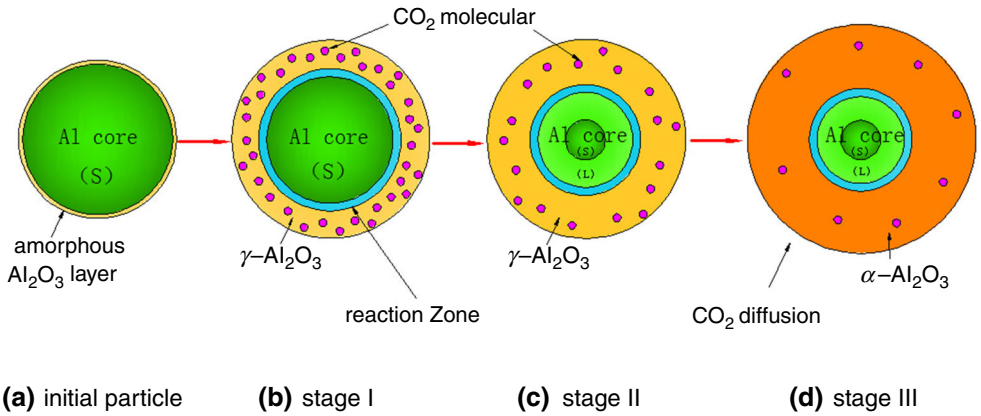

Fig. 6 The reaction of nano-scale Al powder and CO_2 at a low heating rate

bare Al spots will be exposed to the environment and oxidized immediately by CO_2. The above reaction procedure corresponds with the sharp mass increases in Al powder that is shown on TG curve during stage I, and the reaction between nano-scale Al and CO_2 is dominated by chemical kinetics.

At stage II, solid Al transforms into the liquid phase with a little mechanical stress due to a low content of active Al. At the same time, the γ-Al_2O_3 layer that coats on the surface of Al particles grows. This stage is controlled by chemical reaction and diffusion of oxidant. As alumina layer becomes thicker, diffusion of oxidant becomes more difficult.

At stage III, stable α-Al_2O_3 is formed, which results in an abrupt reduction in oxidation rate shown on DTG curve. In this stage, the diffusion from the oxidant to Al core and the oxidation of active Al occur simultaneously. However, what differs from stage II is that the oxide layer on the surface of Al particle is made up of denser α-Al_2O_3, which leads to a more difficult diffusion of oxidant. On the other hand, the alumina layer is much thicker than before, so the reaction of stage III is slower than that of stage II. Thus, the whole reaction of nano-scale Al powder and CO_2 is controlled by the diffusion process.

Thermal reaction mechanisms of micro-scale Al powder

Oxidation of micro-scale Al powder is shown in Fig. 7. During induction stage (20–579 °C), there are no mass gains. With temperature increasing, the thickness of amorphous alumina layer increases. When the temperature gets to the melting point of Al powder, solid Al starts to melt. And the density of active Al which is protected by Al_2O_3 layer decreases from solid Al (2.7 g cm^{-3}) to liquid Al (2.4 g cm^{-3}), and causes a 6 % volume increase in Al core. Volume expansion of Al core in the oxide layer leads to compress pressure within the Al core and the tensile stress on the Al_2O_3 layer. As a result, a pressure gradient generates within the layer and leads to the cracking of the alumina layer, followed by the reaction between Al and CO_2 taking place. The produced CO gas disrupts the oxide shell, leading to formation of some holes. It is the disruption of Al_2O_3 shell and formation of holes that resulting in

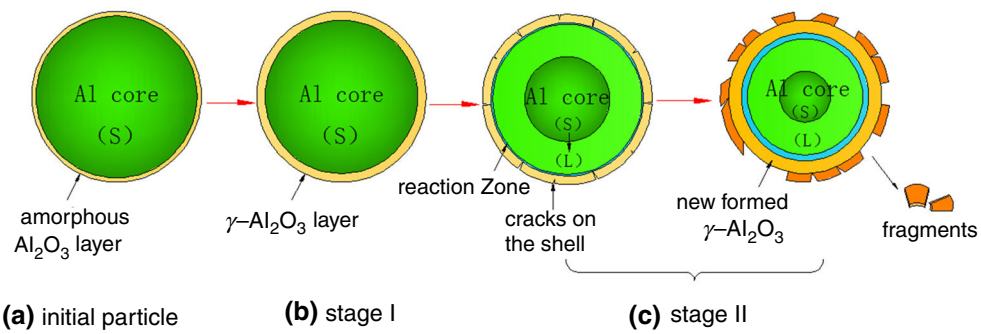

Fig. 7 The reaction of micro-scale Al powder and CO_2 at a low heating rate

an increment of reaction rate, and the mass increases by 74.47 % at stage II.

Conclusions

Thermal reaction mechanisms of nano-scale Al powder are found to differ significantly from micro-scale Al powder by a thermogravimetric analyzer coupled with a differential scanning calorimetry, scanning electron microscopy, and X-ray diffraction.

1. An obvious difference of thermal reaction performance is the oxidation temperature between nano- and micro-scale Al powders. Low-temperature oxidation is prominent for nano-scale Al powder, while high-temperature reaction is the key reaction for micro-scale Al powder. Furthermore, mass gains of micro-scale Al powder are more than those of nano-scale Al powder due to the higher content of active Al. In addition, the oxidation of nano- and micro-scale Al powders in CO_2 atmosphere can be divided into two stages, the induction stage and the mass gains stage. However, there are three mass gains stages for nano-scale Al powder and two mass gains stages for micro-scale Al powder at 20–1400 °C.
2. Some broken alumina fragments with a rough outer surface and holes appear in the thermal reaction products of micro-scale Al powder. However, fragments of oxide shell and the holes are not observed in the thermal reaction products of nano-scale Al powder. And thermal reaction products of nano- and micro-scale Al powders change differently with the temperature increasing. For nano-scale Al powder, γ-Al_2O_3 appears at 600 °C, which is before the melting point of Al. When the temperature reaches 1200 °C, stable α-Al_2O_3 is detected. However, for micro-scale Al powder, the temperature that γ-Al_2O_3 appears is 800 °C, which is higher than the Al melting point. When temperature rises to 1000 °C, γ-Al_2O_3 and θ-Al_2O_3 are found.
3. The thermal reaction process of nano-scale Al powder and CO_2 is controlled by chemical kinetics and diffusion of oxidant at low heating rate. As for micro-scale Al powder, diffusion mechanism is also considered to be the thermal reaction mechanism except the disruption of the oxide shell.

Acknowledgements We greatly appreciate the financial support provided by National Natural Science Foundation of China (Nos. 51376007 and 51206001).

References

1. Liang D, Liu J, Xiao J, Xi J, Wang Y, Zhou J. Effect of metal additives on the composition and combustion characteristics of primary combustion products of B-based propellants. J Therm Anal Calorim. 2015;122:497–508.
2. Mulamba O, Pantoya M. Oxygen scavenging enhances exothermic behavior of aluminum-fueled energetic composites. J Therm Anal Calorim. 2014;116(3):1133–40.
3. Bazyn T, Krier H, Glumac N. Evidence for the transition from the diffusion-limit in aluminum particle combustion. P Combust Inst. 2007;31:2021–8.
4. Bocanegra PE, Chauveau C, Gökalp I. Experimental studies on the burning of coated and uncoated micro and nano-sized aluminium particles. Aerosp Sci Technol. 2007;11(1):33–8.
5. Yan ZX, Deng J, Luo ZM. A comparison study of the agglomeration mechanism of nano- and micrometer aluminum particles. Mater Charact. 2010;61:198–205.
6. Morgan AB, Wolf JD, Guliants EA, Fernando KAS, Lewis WK. Heat release measurements on micron and nano-scale aluminum powders. Thermochim Acta. 2009;488:1–9.
7. Escot Bocanegra P, Davidenko D, Sarou-Kanian V, Chauveau C, Gökalp I. Experimental and numerical studies on the burning of aluminum micro and nanoparticle clouds in air. Exp Therm Fluid Sci. 2010;34:299–307.
8. Dreizin EL. Experimental study of stages in aluminium particle combustion in air. Combust Flame. 1996;105:541–56.
9. Bucher P, Yetter RA, Dryer FL, Parr T, Hanson-Parr D, Viceni E. Flames structure measurement of single, isolated aluminum particles burning in air[C]//Symposium (International) on Combustion. Elsevier. 1996;26(2):1899–908.
10. Friedman R, Maček A. Combustion studies of single aluminum particles[C]//Symposium (International) on Combustion. Elsevier. 1963;9(1):703–12.
11. Badiola C, Gill RJ, Dreizin EL. Combustion characteristics of micron-sized aluminum particles in oxygenated environments. Combust Flame. 2011;158:2064–70.
12. Sarou-Kanian V, Rifflet JC, Millot F, Matzen G, Gökalp I. Influence of nitrogen in aluminum droplet combustion. P Combust Inst. 2005;30:2063–70.
13. Zhu Y, Yuasa S. Effects of oxygen concentration on combustion of aluminum in oxygen/nitrogen mixture streams. Combust Flame. 1998;115:327–34.
14. Rossi S, Dreizin EL, Law CK. Combustion of aluminum particles in carbon dioxide. Combust Sci Technol. 2001;164:209–37.
15. Zhu X, Schoenitz M, Dreizin EL. Aluminum powder oxidation in CO_2 and mixed CO_2/O_2 environments. J Phys Chem C. 2009;113(16):6768–73.
16. Jing Z, Li SF, Kai L, Wang TF, Zhang GC, Wang H, Ma XM. Laser ignition and combustion properties of composite propellant containing nanometal powders. AIAA J. 2006;44(7):1463–7.
17. Sarou-Kanian V, Rifflet JC, Millot F, Gökalp I. Aluminum combustion in wet and dry CO_2: consequences for surface reactions. Combust Flame. 2006;145(1):220–30.
18. Mathieu P, Dubuisson R. Performance analysis of a biomass gasifier. Energy Convers Manage. 2002;43(9):1291–9.
19. Eisenreich N, Fietzek H, del Mar Juez-Lorenzo M, Kolarik V, Koleczko A, Weiser V. On the mechanism of low temperature oxidation for aluminum particles down to the nano-scale. Propell Explos Pyrot. 2004;29:137–45.
20. Sun J, Simon SL. The melting behavior of aluminum nanoparticles. Thermochim Acta. 2007;463:32–40.

21. Pourmortazavi SM, Fathollahi M, Hajimirsadeghi SS, Hosseini SG. Thermal behavior of aluminum powder and potassium perchlorate mixtures by DTA and TG. Thermochim Acta. 2006;443:129–31.
22. Levitas VI, Pantoya ML, Watson KW. Melt-dispersion mechanism for fast reaction of aluminum particles: extension for micron scale particles and fluorination. Appl Phys Lett. 2008;92:201917-3.
23. Levin I, Brandon D. Metastable alumina polymorphs: crystal structures and transition sequences. J Am Ceram Soc. 1998;81(8): 1995–2012.
24. Jeurgens LPH, Sloof WG, Tichelaar FD, Mittemeijer EJ. Thermodynamic stability of amorphous oxide films on metals: application to aluminum oxide films on aluminum substrates. Phys Rev B. 2000;62(7):4707.
25. Trunov MA, Schoenitz M, Dreizin EL. Ignition of aluminum powders under different experimental conditions. Propell Explos Pyrot. 2005;30(1):36–43.
26. Trunov MA, Schoenitz M, Zhu X, Dreizin EL. Effect of polymorphic phase transformations in Al_2O_3 film on oxidation kinetics of aluminum powders. Combust Flame. 2005;140:310–8.